# Open surfaces and gauge-invariant Ising models

Giuseppe Gonnella
*Dipartimento di Fisica dell'Università di Bari, I-70126 Bari, Italy*
*and Istituto Nazionale di Fisica Nucleare, Sezione di Bari, via Amendola 173, I-70126 Bari, Italy*

J. M. J. van Leeuwen
*Instituut-Lorentz, Nieuwsteeg 18, 3211 SB Leiden, The Netherlands*
(Received 8 August 1994; revised manuscript received 15 February 1995)

We study the phase diagram of $Z(2)$ gauge-Higgs models in three dimensions. These models can describe the dual lattice of open surfaces with an energy depending on the area and on the defect length. By perturbative methods, we map the gauge systems onto Ising models with many interactions, for which we determine the transition lines. We discuss how tricritical points could arise on these lines. In particular, we consider the cubic and the fcc lattice; on the dual lattice of the fcc, the surfaces are self-avoiding. We also discuss the effect of other surface energies on the phase diagram of the gauge-Higgs model.

PACS number(s): 05.50.+q, 11.15.Ha, 68.10.−m

## I. INTRODUCTION

This paper concerns the phase diagram of the so-called $Z(2)$ gauge-Higgs model [1] and its relation to random surfaces and, in particular, to surfactant membranes. Random surfaces are statistical bidimensional objects fluctuating in a three-dimensional space. They have been proven to provide useful descriptions of equilibrium properties of a large variety of physical systems [2]. Among them, ensembles of fluid films display a particularly interesting statistical behavior. They exist or can be realized in different ways. In mixtures of oil, water, and surfactant, the surfactant molecules form interfaces between oil and water, with very different spatial configurations, depending on the temperature, the presence of other substances, or other parameters [3]. In aqueous surfactant solutions, the amphiphilic molecules form bilayer membranes that still self-organize in many different structures. If the surfactant solutions are sufficiently dilute, the interfaces strongly fluctuate and tend to assume any possible topology. For example, disordered evolutions of bicontinuous structures (sometimes called *sponge phases*) [4], where the interfaces divide all the volume into two intertwined connected regions, have been experimentally observed in both of the above systems [5,6].

The lack of constraints on topologies suggests the use of lattice models for the description of these systems. In three-dimensional Ising models one can consider the closed interfaces separating regions of equal spins. Each time two nearest-neighboring sites have different signs, an interface is drawn on the dual plaquette, and the total area of the interfaces is given by $S=\sum_{\langle ij\rangle}(1-s_i s_j)/2$, where the $s_i$'s are spin variables defined on the sites of a generic three-dimensional lattice and the sum is over all nearest-neighbor pairs. Therefore only the area is weighted in the surface representation of the Ising model. A more realistic description of an ensemble of fluid films can be formulated by also attributing a weight to the bendings. Moreover, depending on the lattice geometry, the interfaces can be self-intersecting in the sense that more than three plaquettes of the dual lattice share a dual link. Therefore, in such cases, it is realistic to also attribute a weight to the self-intersections. For example, in the cubic lattice, given a spin configuration with the corresponding interface description on the dual lattice, a bending corresponds to a pair of adjacent plaquettes belonging to the interfaces that are at a right angle, while a self-intersection is a dual link shared by four plaquettes of the interface configuration. The total number of bendings and self-intersections can be weighted by considering a spin model with nearest-neighbor, next-nearest-neighbor, and plaquette interactions [7]. The phase diagram of this model includes bicontinuous ordered phases and a sponge region with only short-range order [7,8].

If one wishes to describe surfaces that also have defects, like free-edges or seams, it is necessary to introduce different Ising variables $U_{ij}$ defined on the links of a lattice. When $U_{ij}$ is equal to $-1$, we assume that the dual plaquette of the link $\langle ij\rangle$ is occupied by a surface, while, when $U_{ij}$ is equal to $+1$, there is no surface on that plaquette. Therefore a configuration of the variables $U_{ij}$ can describe a generic open surface configuration with an area given by $\sum_{\langle ij\rangle}(1-U_{ij})/2$. The defects consist of dual links that belong to an odd number of plaquettes occupied by surfaces; see an example in Fig. 1. If $U_{\mathcal{P}}$ denotes the product of the variables $U_{ij}$ along the links bounding a plaquette $\mathcal{P}$ of the original lattice, the quantity $\sum_{\mathcal{P}}(1-U_{\mathcal{P}})/2$ represents the total length of defects. The open surface model, where the area and the defects are weighted, is the gauge-Higgs system

$$Z(\beta_1,\beta_{\mathcal{P}})=\sum_{\{U_{ij}\}}\exp\left[\beta_1\sum_{\langle ij\rangle}U_{ij}+\beta_{\mathcal{P}}\sum_{\mathcal{P}}U_{\mathcal{P}}\right], \qquad (1.1)$$

which in the gauge-invariant version reads

 

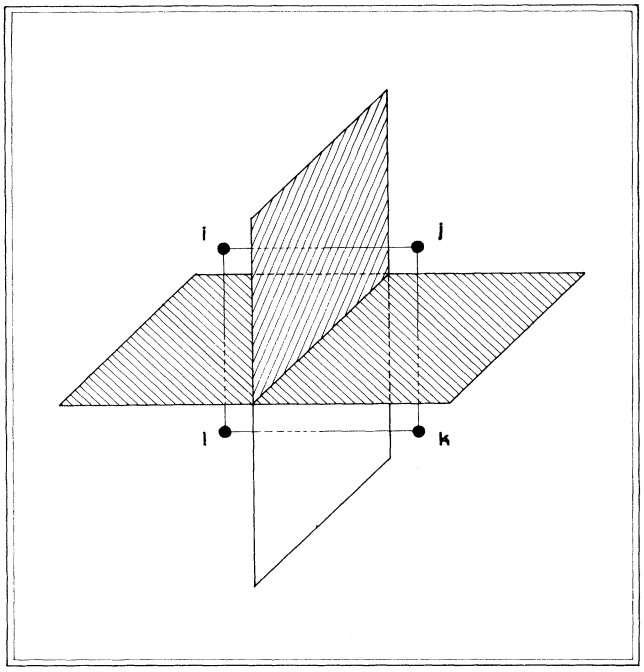


FIG. 1. Local configuration representing a *seam* defect. The three dashed plaquettes belong to some surface; $U_{lk}$ is the only positive link variable.

$$Z(\beta_1,\beta_{\mathcal{P}})=\frac{1}{2^N}\sum_{\{\sigma_i\},\{U_{ij}\}}\exp\left[\beta_1\sum_{\langle ij\rangle}\sigma_i U_{ij}\sigma_j+\beta_{\mathcal{P}}\sum_{\mathcal{P}}U_{\mathcal{P}}\right], \tag{1.2}$$

where the $\sigma_i$'s are Ising variables defined on the $N$ lattice sites. The equivalence between the two expressions can be easily seen: $2^N$ equivalent copies of the original system (1.1) are considered; for each of them the variables $U_{ij}$ are written as $\sigma_i\tilde{U}_{ij}\sigma_j$, covering all the possible configurations of the variables $\sigma_i$. The model (1.2) is gauge invariant in the sense that its Hamiltonian is left unchanged by the simultaneous transformations $U_{ij}\to\gamma_i U_{ij}\gamma_j$ and $\sigma_i\to\gamma_i\sigma_i$, where $\gamma_i=\mp 1$. It can be considered as the discrete version of the $Z(2)$ gauge model coupled with a Higgs field [9].

The phase diagram of this model, in the cubic lattice at $\beta_4\equiv\beta_{\mathcal{P}}>0$, is known from numerical simulations [10]. Simple approximative methods do not give the correct topology of the phase diagram [11]. Its description in terms of membrane configurations is given in [12]. The model has been numerically studied in [13] at negative gauge couplings, while the mean-field calculation of the phase diagram and its surface description have been carried out in [14]. A correct analytical description of the phase diagram still is an open question.

In the present paper we focus our attention on some aspects of the phase diagram of the model (1.1), known only by numerical simulations [10] so far. In Fig. 2 the phase diagram for the cubic lattice is shown, as it comes out from our calculations. The transition lines start at the critical Ising points ($\beta_4=\infty$, $\beta_1=\beta_c$), where $\beta_c=0.2217$ is the inverse Ising critical temperature [15], and at ($\beta_4=\tilde{\beta}_c=0.7613$, $\beta_1=0$), where

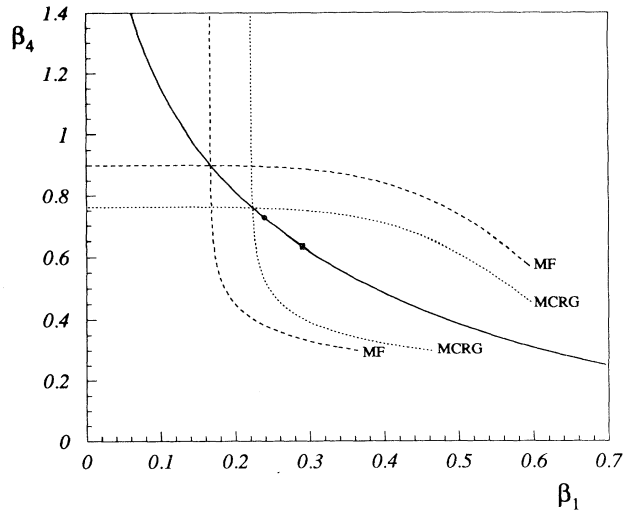


FIG. 2. Phase diagram of the $Z(2)$ gauge-Higgs model in the cubic lattice. The continuous line is the self-dual line, while the dashed lines are the critical lines calculated by the mean-field and Monte Carlo renormalization-group approximations. The dot and the square represent the triple point and the critical point, as coming out of Monte Carlo simulations [10].

$$\tilde{\beta}=-\tfrac{1}{2}\ln\tanh\beta \tag{1.3}$$

is the duality transformation exchanging the low- and the high-temperature regimes. In this paper we predict the shape of the transition lines with better precision than was reached in earlier calculations, and we give arguments for the existence of tricritical points on these lines, which so far have only been numerically predicted. These results are obtained by mapping the model at extreme but finite values of the parameters onto Ising models with many interactions, and then using Monte Carlo renormalization-group results and mean-field approximations.

The paper is organized as follows. In the next section, our results about the $Z(2)$ gauge-Higgs system in the cubic lattice will be derived. In Sec. III we study the same system on the fcc lattice, where self-avoiding surfaces in quite a natural way can be realized. In our approximations, we will discuss the effect of lattice symmetries on the phase diagram of the model. In Sec. IV we summarize and discuss our results in relation to membrane systems; we also make some comments on the effects of other interactions, representing, for example, surface curvature or distinct energies for different defects, on the phase diagram of Fig. 2.

## II. PHASE DIAGRAM OF THE $Z(2)$ GAUGE-HIGGS MODEL IN THE CUBIC LATTICE

The model (1.1) was introduced in [1] as a generalization of the Ising model. Its gauge-invariant version has been studied in the context of lattice gauge theories for

strong interactions [16]. An introductory general description of the phase diagram will be briefly given.

In the cubic lattice, the model exhibits the important property of self-duality [1,17], which means that it can be expressed on the dual lattice as the same model with interaction parameters given by

$$\beta_1^{\mathcal{D}}=\tilde{\beta}_4, \quad \beta_4^{\mathcal{D}}=\tilde{\beta}_1 . \tag{2.1}$$

Therefore the phase diagram has to be symmetric with respect to the *self-dual line,* drawn as a continuous line in Fig. 2, which is the line left invariant under the transformations (2.1).

The model is trivial at $\beta_4=0$, where there is no transition. It can also be shown that there is no transition at finite small values of $\beta_4$, and that this region is thermodynamically connected to the region of large $\beta_1$ and any $\beta_4$ [18]. The limit cases $\beta_4=\infty$ and $\beta_1=0$ can also be easily discussed. At $\beta_4=\infty$, the products $U_{\mathcal{P}}$ have to assume the value $+1$ for each plaquette. This constraint can be solved by setting for each link $U_{ij}=s_i s_j$ [19], where the $s_i$'s are Ising variables defined on the sites. Therefore the model becomes equivalent to the Ising model and there is a second-order transition at $\beta_1\approx 0.2217$, which is related by Eq. (1.3) to the transition point along the axis $\beta_1=0$. On this axis the model can be directly proven to be dual to the three-dimensional Ising model [1] (see Appendix A).

It can be argued that the critical points at $\beta_4=\infty$ and $\beta_1=0$ are stable when moving inside the phase diagram at finite values of the parameters [1,18]. The corresponding critical lines, as coming out of our calculations, are drawn in the phase diagram of Fig. 2. However, the numerical simulations of Ref. [10] show a first-order behavior for these lines just before they meet on the self-dual line, thus suggesting the existence of tricritical points $T$ and $T'$, where the continuous transitions change over in first-order behavior. Actually, as coming from simulations, the point where the lines meet is a triple point where also a first-order line starts ending at a critical point $C$, see Fig. 2. In the following we shall concentrate on the study of the two transition lines starting from $\beta_4=\infty$ and $\beta_1=0$.

### A. Small $\beta_1$

The term proportional to $\beta_1$ formally looks like a magnetic field. However, in locally gauge-invariant theories any local quantity that is not gauge invariant (as $U_{ij}$) has a vanishing mean at any temperature [20]. Therefore the parameter $\beta_1$ does not act as a symmetry-breaking magnetic field and there is no reason for the transition at $\beta_1=0$ to disappear at finite values of $\beta_1$ [1]. In the following we shall study the model in this region, expanding it as an Ising model with an increasing number of interactions.

We start from the expression (1.2) and integrate over the variables $\sigma_i$, thus obtaining the expansion

$$\mathcal{Z}(\beta_1,\beta_4)=(\cosh\beta_1)^{N_{\langle\rangle}} \times \sum_{\{U_{ij}\}} \exp\left[\beta_4 \sum_{\mathcal{P}} U_{\mathcal{P}}\right] \sum_{\Gamma} (\tanh\beta_1)^{L(\Gamma)} \times \prod_{\langle ij\rangle\in\Gamma} U_{ij} , \tag{2.2}$$

where $N_{\langle\rangle}=3N$ is the number of links in a cubic lattice, $L(\Gamma)$ is the length of a closed loop $\Gamma$, and the sum includes all possible closed loops. The smallest loop is a plaquette, so that the lowest order term of the expansion can be seen as a change of the parameter $\beta_4$ into $\beta_4^{\text{eff}}=\beta_4+(\tanh\beta_1)^4$, shifting the transition from $\beta_4=\tilde{\beta}_c$ to $\beta_4=\tilde{\beta}_c-(\tanh\beta_1)^4$, as was argued by Fradkin and Shenker in [18]. Here we study the effect of larger loops on the Ising transition. [Equation (2.2) can be directly obtained from (1.1) on observing that the high-temperature expansion with respect to $\beta_1$ can include only gauge-invariant quantities.]

An effective Hamiltonian can be obtained from (2.2) by exponentiating the loop expansion. First we use for an arbitrary loop $\Gamma$ the identity [17] (see also Appendix A)

$$\sum_{\{U_{ij}\}} \exp\left[\beta \sum_{\mathcal{P}} U_{\mathcal{P}}\right] \prod_{\langle ij\rangle\in\Gamma} U_{ij} = (2\sinh 2\beta)^{N_{\mathcal{P}}/2} \sum_{\{s_i\}} \exp\left[\sum_{\langle ij\rangle} \beta_{ij} s_i s_j\right] . \tag{2.3}$$

Here the $s_i$'s are spins located on the dual lattice, and the sum over $\langle ij\rangle$ on the right-hand side is over links in the dual lattice (while the links on the left-hand side are on the original lattice). The values of $\beta_{ij}$ are related to the loop $\Gamma$ as follows. We choose a minimal set of plaquettes $\mathcal{S}_\Gamma$ that have $\Gamma$ as a boundary. (It can happen that there are many minimal surfaces for one contour. In that case they all have to be taken into account in order to get a symmetric spin Hamiltonian.) When a dual link crosses such a plaquette $\beta_{ij}=-\tilde{\beta}$ and $\beta_{ij}=\tilde{\beta}$ otherwise. $N_{\mathcal{P}}$ is the total number of plaquettes in the lattice.

Second we write for every factor with $\beta_{ij}=-\tilde{\beta}$,

$$e^{-\tilde{\beta} s_i s_j}=e^{\tilde{\beta} s_i s_j}(\mathcal{C}-\mathcal{S} s_i s_j) , \tag{2.4}$$

where

$$\mathcal{C}=\cosh 2\tilde{\beta} , \tag{2.5a}$$

$$\mathcal{S}=\sinh 2\tilde{\beta} . \tag{2.5b}$$

Then all loop contributions have the same exponential factor $\exp(\tilde{\beta}\sum_{\langle ij\rangle} s_i s_j)$ and a loop-dependent product

$$P_\Gamma=\prod_{\langle ij\rangle\in\tilde{\mathcal{S}}_\Gamma} (\mathcal{C}-\mathcal{S} s_i s_j) , \tag{2.6}$$

where $\tilde{\mathcal{S}}_\Gamma$ is the set of links dual to the surface $\mathcal{S}_\Gamma$. We illustrate the result so far with the loops to order $(\tanh\beta_1)^6$. The expansion (2.2) can be written as

$$Z(\beta_1,\beta_4)\sim\sum_{\{s_i\}}\exp\left[\tilde{\beta}_4^{\text{eff}}\sum_{\langle ij\rangle}s_is_j\right]\left\{1+(\tanh\beta_1)^6\sum_{\Gamma_6}\prod_{\langle ij\rangle\in\tilde{S}_\Gamma}(\mathcal{C}-\mathcal{S}s_is_j)+\cdots\right\}, \tag{2.7}$$

where

$$\beta_4^{\text{eff}}=\beta_4+(\tanh\beta_1)^4 \tag{2.8}$$

and $\mathcal{C}$ and $\mathcal{S}$ are functions of $\tilde{\beta}_4^{\text{eff}}$. There are three loops at sixth order that are depicted in Fig. 3 together with their dual spins. The last step is the exponentiation of the factor enclosed in brackets, which leads to the representation

$$\begin{aligned}Z(\beta_1,\beta_4)&=\sum_{\{s_i\}}e^{\mathcal{H}(s_i)}\ ,\\ \mathcal{H}\{s_i\}&=\text{const}+\mathcal{J}_{\text{NN}}\sum_{\text{NN}}s_is_j+\mathcal{J}_{\text{NNN}}\sum_{\text{NNN}}s_is_j\\ &\quad+\mathcal{J}_{\text{pla}}\sum_{\text{pla}}s_js_ks_ls_l+\mathcal{J}_{\text{cor}}\sum_{\text{cor}}s_is_js_ks_l\ ,\end{aligned} \tag{2.9}$$

where the interactions are between nearest neighbors, next nearest neighbors, the four spins of a plaquette, and the four spins that form a corner (see Fig. 4), and

$$\mathcal{J}_{\text{NNN}}=\tilde{\beta}_4^{\text{eff}}-4(\tanh\beta_1)^6(3\mathcal{C}\mathcal{S}+\mathcal{C}^2\mathcal{S})\ , \tag{2.10a}$$

$$\mathcal{J}_{\text{NNN}}=2(\tanh\beta_1)^6(\mathcal{S}^2+\mathcal{C}\mathcal{S}^2)\ , \tag{2.10b}$$

$$\mathcal{J}_{\text{pla}}=2(\tanh\beta_1)^6\mathcal{S}^2\ , \tag{2.10c}$$

$$\mathcal{J}_{\text{cor}}=-\tfrac{1}{2}(\tanh\beta_1)^6\mathcal{S}^3\ . \tag{2.10d}$$

The convenience of the representation (2.9) and (2.10) is that spin models can be more easily studied. We have used Monte Carlo renormalization-group results for the critical surface of the model (2.9). In this method the system is simulated, with the coupling as given by (2.10). At the same time renormalized systems are deduced by means of a majority rule applied to blocks. The cross correlations between the original spins and the block spins yield the flow matrix for the renormalization trajectory. From the flow towards the fixed point the critical surface can be determined. The vector describing the orientation of the critical surface at the nearest-neighbor point is (1.000,2.652,0.788,2.490) [21] with the components referring to the four couplings of the Hamiltonian (2.9) in the same order as in Eqs. (2.10). By inserting the expressions (2.10) into the equation of the critical surface, one gets the critical line drawn in Fig. 2.

A new feature coming out of these calculations is that loops larger than a plaquettes in (2.2) are also relevant to the nature of the transition. On the dual lattice these loops correspond to many-spin interactions whose effects on the transition can be understood, for example, by considering the mean-field expression of the free-energy of the model (2.9). Its expansion at small values of the average magnetization $m$ is given by

$$\begin{aligned}\frac{\gamma}{k_BTN}\approx(\tfrac{1}{2}&-3\{\beta_4^{\text{eff}}-4\mathcal{S}(\tanh\beta_1)^6[\mathcal{C}(3+\mathcal{C})\\ &-\mathcal{S}(1+\mathcal{C})]\})m^2\\ &+[\tfrac{1}{12}-2\mathcal{S}^2(\tanh\beta_1)^6(3-2\mathcal{S})]m^4+\tfrac{1}{32}m^6\ .\end{aligned} \tag{2.11}$$

The curve where the coefficient of the quadratic term is zero gives the critical line of the model (2.9) in the mean-field approximation. On this line the point where the coefficient of the quartic term is also zero is a tricritical point. Its position is at $\beta_1^{\text{tricr}}=0.936$. Albeit rather far from expected, this can be considered an analytical argument for the existence of a tricritical point in the self-dual Higgs-gauge model.

### B. Large $\beta_4$

The results obtained at small $\beta_1$ can be mapped by self-duality to the region with large $\beta_4$. This gives the line starting at $\beta_4=\infty$ in Fig. 2. However, also in this region the model (1.1) can be expanded as a spin model with an increasing number of interactions that, at each order of the expansion, are the same as those of the previ-

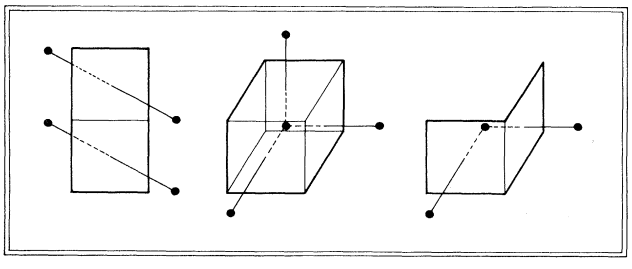

FIG. 3. Loops of length 6 in the cubic lattice. The dots represent the dual spins interacting through Eq. (2.6). There are two minimal surfaces having the loop in the middle as a boundary; only the spins dual to one of these surfaces are drawn.

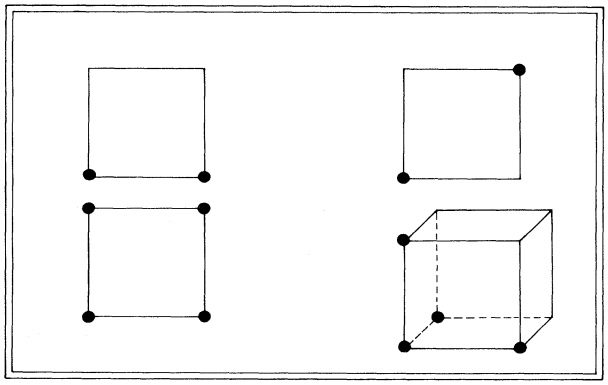

FIG. 4. Four clusters of spins interacting in the Hamiltonian (2.9).

ous section. Since we shall later use both expansions in cases when they are not equivalent anymore, we show here how the expansion at large values of $\beta_4$ can be obtained.

We already mentioned that in the limit $\beta_4 \to \infty$ the model is equivalent to an Ising model with interaction parameter $\beta_1$. When $\beta_4$ becomes finite but is still large, excitations with respect to the ground state with $U_{\mathcal{P}}=+1$ for each plaquette have to be considered. They consist of configurations with a few frustrated plaquettes ($U_{\mathcal{P}}=-1$). A low-temperature expansion can be constructed as follows. The number of frustrated plaquettes for each cube has to be even; therefore, the loops made by dual links to the frustrated plaquettes are closed. Hence, the low-temperature expansion can be interpreted as an expansion of closed loops on the dual lattice. For each of these loops we take the surface made of plaquettes of the dual lattice that has minimal area and that loop as a boundary. The dual links to each plaquette of this surface are on the original lattice, and we call them *frustrated links.* Now we observe that, for each loop, the original Hamiltonian is restricted by the constraint that all the plaquettes are not frustrated, except the dual plaquettes to the links of that loop. This constraint can be solved by putting $U_{ij}=-s_i s_j$ for the frustrated links, and $U_{ij}=+s_i s_j$ for all the others. Then the relation (2.4) with $\beta_1$ instead of $\tilde{\beta}$ can be used for the frustrated links, and at large $\beta_4$ the model results in an Ising model with many interactions. Since the result is the dual version of the one obtained in the previous section, we show the above procedure in considering only the first term of the expansion, which is a loop of four links, corresponding to an excitation with four frustrated plaquettes, if periodic boundary conditions are assumed. At large $\beta_4$ the model (1.1) can be written as

$$Z(\beta_1,\beta_4)=\frac{e^{\beta_4 N_{\mathcal{P}}}}{2}\sum_{\{s_i\}}\exp\left[\sum_{\langle ij\rangle}\beta_1 s_i s_j\right]\left\{1+e^{-8\beta_4}\sum_{\langle ij\rangle}(\cosh 2\beta_1 - s_i s_j \sinh 2\beta_1)+\cdots\right\}$$
$$=\frac{e^{\beta_4 N_{\mathcal{P}}}}{2}\exp(N_{\langle\rangle}e^{-8\beta_4}\cosh 2\beta_1)\sum_{\langle s_i\rangle}\exp\left[\sum_{\langle ij\rangle}(\beta_1 - e^{-8\beta_4}\sinh 2\beta_1)s_i s_j\right]+\cdots . \tag{2.12}$$

Therefore, as expected, the first term of the expansion simply renormalizes the Ising coupling, giving a transition line

$$\beta_1=\beta_c+e^{-8\beta_4}\sinh 2\beta_1 , \tag{2.13}$$

which is the dual expression of Eq. (2.8) with $\beta_4^{\text{eff}}=\tilde{\beta}_c$.

## III. GAUGE-HIGGS MODEL ON THE fcc LATTICE

In this section we study the model (1.1) on the fcc lattice, which is an especially interesting case to be studied, since, due to the special geometry, it can describe surfaces that become self-avoiding when defects have a large energy cost. Indeed, the dual lattice of the fcc lattice (see Fig. 5) has links shared only by three plaquettes. Thus, in the closed surface limit $\beta_3\equiv\beta_{\mathcal{P}}=\infty$, only 2 or 0 plaquettes for each dual link are occupied by surfaces, and intersections are forbidden. (Closed self-avoiding surfaces resulting from high-temperature expansion of a gauge model on the dual lattice of the fcc lattice have been considered in [23].)

The model explicitly reads

$$Z(\beta_1,\beta_3)=\sum_{\{U_{ij}\}}\exp\left[\beta_1\sum_{\langle ij\rangle}U_{ij}+\beta_3\sum_{\Delta}U_{\mathcal{P}}\right] . \tag{3.1}$$

On the axis $\beta_1=0$ it is equivalent to the nearest-neighbor Ising model on the dual lattice of the fcc lattice (see Appendix A). Therefore there is a transition at $\beta_3=\tilde{\beta}_c=-\frac{1}{2}\ln\tanh\beta_c$, where $\beta_c$ is the critical Ising parameter for the dual lattice. The mean-field estimate for this critical value is $\beta_c=\frac{1}{4}\sqrt{2}$ [see Eq. (B2) and the following]. At small $\beta_1$, the same procedure of Sec. II A can be used. A gauge-invariant expansion as that of Eq. (2.2) can be written, where now the closed loops are on the edges of the fcc lattice. At the next to the lowest order of this expansion, the partition function is given by

$$Z(\beta_1,\beta_3)=(\cosh\beta_1)^{N_{\langle\rangle}}\sum_{\{U_{ij}\}}e^{\beta_3^{\text{eff}}\sum_{\Delta}U_{\mathcal{P}}}\left\{1+(\tanh\beta_1)^4\sum_{\Gamma_4}\prod_{\langle ij\rangle\in\Gamma_4}U_{ij}+o[(\tanh\beta_1)^6]\right\} , \tag{3.2}$$

where the contours $\Gamma_4$ of length 4 are drawn in Fig. 6 and

$$\beta_3^{\text{eff}}=\beta_3+(\tanh\beta_1)^3 . \tag{3.3}$$

The expression (3.2) can be written on the dual lattice as a spin model with a Hamiltonian given by

$$\mathcal{H}\{s_i\}=[\tilde{\beta}_3^{\text{eff}}-\tfrac{15}{2}(\tanh\beta_1)^4\mathcal{C}\mathcal{S}]\sum_{\text{NN}}s_i s_j+2(\tanh\beta_1)^4\mathcal{S}^2\sum_{\text{NNN}}s_i s_j+(\tanh\beta_1)^4\mathcal{S}^2\sum_{\text{3rd N}}s_i s_j+2(\tanh\beta_1)^4\mathcal{S}^2\sum_{\text{pla}}s_i s_j s_k s_l , \tag{3.4}$$

where the sums are, respectively, over nearest neighbors, next-nearest neighbors, third neighbors, and plaquettes, and $\mathcal{C}$ and $\mathcal{S}$ are functions of $\tilde{\beta}_3^{\text{eff}}$. In Appendix B the critical line of this Hamiltonian is given in the mean-field approximation [see Eq. (B5)] with a tricritical point at $\beta_1=0.745$.

We consider now the limit $\beta_3\to\infty$. Only configurations where the product $U_{ij}U_{jk}U_{ki}$ is equal to $+1$ for each triangle are allowed in this limit. Therefore the model (3.1) can be written as a nearest-neighbor Ising model on the fcc lattice, with a second-order transition at $\beta_1=\frac{1}{12}$ in the mean-field approximation. (A better result for this transition is $\beta_1=0.1017$ [15]; here, we will consider the mean-field approximated value, since we want to use that together with the only other available mean-field results.) When $\beta_3$ is still large but finite, configurations with few frustrated triangles also have to be taken into account. As in Sec. II B, they can be represented by closed loops on the dual lattice made by links normal to the frustrated triangles. At the next to the lowest order of this expansion, one has to consider the loops of Fig. 7, and the procedure discussed in Sec. II B gives

$$Z(\beta_1,\beta_3)=\frac{e^{\beta_3 N_\Delta}}{2}\sum_{\{s_i\}}\left\{\exp\left[\beta_1\sum_{\langle ij\rangle}s_is_j\right]+e^{-8\beta_3}\sum_{\langle mn\rangle}\exp\left[-\beta_1 s_m s_n+\sum_{\langle ij\rangle\neq\langle mn\rangle}\beta_1 s_i s_j\right]\right.$$
$$+e^{-12\beta_3}\sum_{C_1}\exp\left[-\beta_1(s_l s_m+s_l s_n)+\sum_{\langle ij\rangle\neq\langle lm\rangle,\langle ln\rangle}\beta_1 s_i s_j\right]$$
$$\left.+e^{-12\beta_3}\sum_{C_2}\exp\left[-\beta_1(s_l s_m+s_l s_n+s_l s_p)+\sum_{\langle ij\rangle\neq\langle lm\rangle,\langle ln\rangle,\langle lp\rangle}\beta_1 s_i s_j\right]+\cdots\right\}, \tag{3.5}$$

where the sums are over nearest neighbors and over the clusters $C_1$ and $C_2$ of Fig. 7. The resulting spin Hamiltonian reads

$$\mathcal{H}\{s_i\}=\mathcal{J}_{\text{NN}}\sum_{\text{NN}}s_is_j+\mathcal{J}_{C_2}\sum_{C_2}s_is_js_ks_l \tag{3.6}$$

with

$$\mathcal{J}_{\text{NN}}=[\beta_1-e^{-8\beta_3}\mathcal{S}+e^{-12\beta_3}(-8\mathcal{C}\mathcal{S}+4\mathcal{S}^2-4\mathcal{C}^2\mathcal{S}+4\mathcal{C}\mathcal{S}^2)], \tag{3.7a}$$

$$\mathcal{J}_{C_2}=-e^{-12\beta_3}4\mathcal{S}^3. \tag{3.7b}$$

Here $\mathcal{C}$ and $\mathcal{S}$ are functions of $\beta_1$, and (3.7a) and (3.7b) refer, respectively, to nearest neighbors and clusters $C_2$. The corresponding mean-field expression of the site free energy $\gamma$ is given by

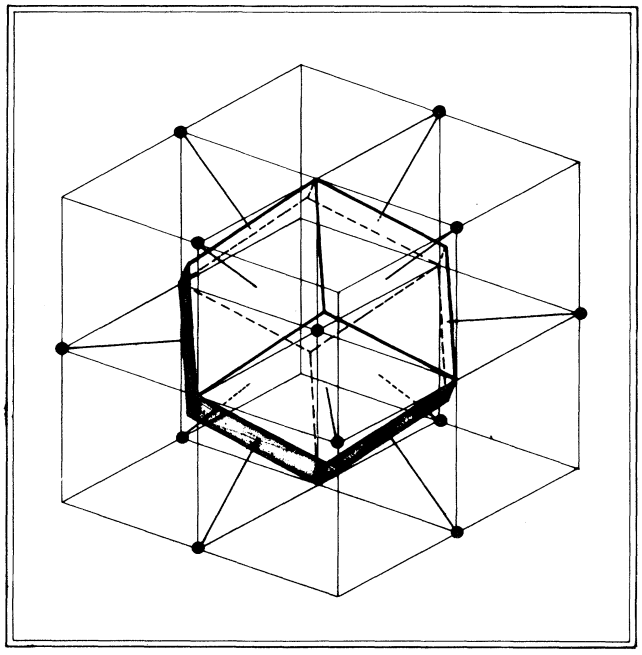

FIG. 5. Fcc lattice with a cell of dual lattice. The dots are the lattice points of the fcc lattice (see [22]).

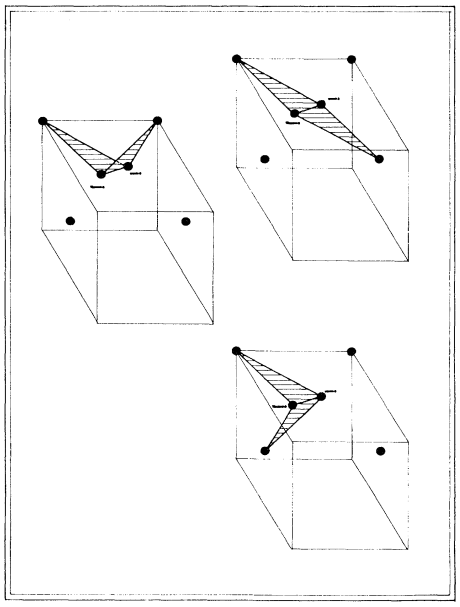

FIG. 6. Three kinds of contours of length on the fcc lattice for each link $\langle ij\rangle$.

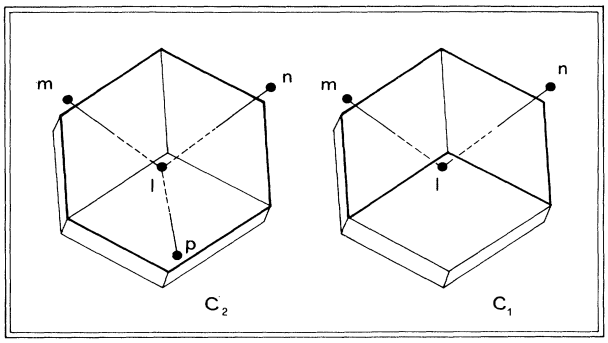


FIG. 7. Loops of length 6 on the dual of the fcc lattice with their dual spins. The spins $l,m,n,p$ and $l,m,n$ form, respectively, the clusters denoted $C_2$ and $C_1$ in the main text.

$$\beta\gamma \approx (\tfrac{1}{2}-6\mathcal{J}_{\mathrm{NN}})m^2+(\tfrac{1}{12}-2\mathcal{J}_{C_2})m^4+\tfrac{1}{32}m^6+\cdots , \tag{3.8}$$

where $m$ is the approximated average of a spin $s_i$. The equation $\mathcal{J}_{\mathrm{NN}}=\frac{1}{12}$ gives the critical line at large $\beta_3$. This line intersects the one starting from the axis $\beta_1=0$ at the triple point $\beta_1\approx 0.08$, $\beta_3\approx 0.87$. The overall picture is similar to that of Fig. 2.

However, there could be a difference with the cubic case with regard to the tricritical points. At this level of approximation, in the fcc lattice, due to the fact that the coefficient of the quartic term in (3.8) is positive definite, there is no indication of a first-order behavior on the vertical transition line. Therefore, while the global topology of the phase diagram of the model (1.1) is expected to be the same for any three-dimensional lattice, it is difficult to say whether the existence of tricritical points is a general aspect of the phase diagram or not.

## IV. DISCUSSION AND CONCLUSIONS

In the previous sections we have analyzed the phase diagram of the three-dimensional $Z(2)$ gauge-Higgs model in different lattices. We have shown how systematic expansions can be used to predict the shape of the transition lines in the neighborhood of the Ising critical points at $\beta_1=0$ and $\beta_P=\infty$. By also using our results in regions not very close to the Ising critical points, we find that the two critical lines exhibit a very low curvature before intersecting at some point. Tricritical points have been found on these critical lines beyond the intersection point, far outside the region where our expansions can be relied on. This means that our results may suggest interesting ideas about the behavior of the system, but that a better approximation is needed for studying the whole phase diagram of gauge-Higgs models. (For a discussion about the failure of the mean-field approximation in describing the correct topology of the phase diagram, see, e.g., Ref. [11].) In the following we will discuss in more detail our results for the cubic and the fcc lattices.

In the cubic lattice the point of intersection between the two critical lines is on the self-dual line at $\beta_1=0.223$. This value has to be compared with the position of the triple point at $\beta_1\approx 0.24$ coming out from simulations [10]. Our expansions are unable to uncover the first-order line emerging from the triple point onto the self-dual line. The existence of the first-order line is intimately related with the appearance of tricritical points (as borne out by simulations) on the critical lines, changing the nature from a continuous transition to a first-order transition very close to the triple point. The tricritical points are at $\beta_1\approx 0.21$ and at $\beta_1\approx 0.23$ on the horizontal and on the vertical line, respectively. From our expansions we get interaction terms that suggest the existence of tricritical points. In a mean-field approximation they appear for values beyond the triple point and are therefore irrelevant, as the phase transition terminates at the triple point. The application of the cluster variation method, which is a more accurate approximation than the mean-field approximation, does not change in a significant way the position of tricritical points [24]. Therefore the wrong position of tricritical points in our estimate is probably due to having considered only the first two terms in the loop expansion (2.2).

The situation is less clear for other lattices. The fcc lattice shows two intersecting critical lines, but the evidence for tricritical points on these critical lines is weaker. On the line emanating from the $\beta_1=0$ Ising point, one finds in the mean-field approximation a tricritical point that is again beyond the triple point, as in the cubic case. On the other critical line one does not find a tricritical point in the mean-field approximation. Whether the geometry of the lattice is relevant for the existence of the tricritical point is a question that is worthy of further study.

Finally we briefly discuss a generalization of the gauge-Higgs model. We have studied the model (1.1) in relation to a statistical description of open membrane systems. Therefore an interesting question is the evolution of the phase diagram of Fig. 2 when other surface energies are considered. It is possible to define gauge models describing open surfaces with curvature and other interactions by introducing new non-gauge-invariant terms in (1.1) [7]. In these generalized models, expansions close to the $\beta_4$ axis and to the point $\beta_4\to\infty$ can still be performed. The resulting spin interactions are the same as in Sec. II, but with different factors. Therefore in these extreme regions of the phase diagram the transition lines can be studied by our methods. For positive couplings, the continuous character of the transition close to the $\beta_4$ axis will not change. However, the transition can become of first order in the limit $\beta_4=\infty$ when other interactions are considered. For example, if one considers a model of open surfaces where the curvature and the intersections are also weighted, in the limit $\beta_4=\infty$ one gets a spin model [7] that exhibits, in some range of the parameters, a first-order paramagnetic-ferromagnetic transition.

In the region close to the limit $\beta_P\to\infty$, surfaces have a few defects. Here the transition can be interpreted as a symmetry-breaking transition in the sponge region where the volumes *inside* and *outside* the surfaces becomes different [12,25]. We have shown in Sec. II B that an or-

der parameter can be defined to describe this transition. The *inside-outside* transition, first studied in [25], has been experimentally observed in systems where the concentration of defects is negligible [26]. From the perspective of considering physical systems that provide an experimental counterpart of gauge models, the possibility of taking into control the concentration of defects would be of great interest.


## ACKNOWLEDGMENTS

The authors thank H.W. J. Blöte and J. Heringa for making available to them the critical point parameters of the $d=3$ Ising model. G.G. has the pleasure of thanking the members of the Lorentz Institute for their kind hospitality. He also warmly thanks Amos Maritan and Alessandro Pelizzola for discussions about the subject of this paper.


## APPENDIX A: DUALITY BETWEEN PURE GAUGE AND ISING MODELS

For the convenience of the reader we sketch here a proof of the equivalence between pure gauge models and three-dimensional Ising models on the dual lattice, which is used in (2.3). We start from

$$Z(\beta_{\mathcal{P}})=\sum_{\{U_{ij}\}}\exp\left[\beta_{\mathcal{P}}\sum_{\mathcal{P}}U_{\mathcal{P}}\right], \tag{A1}$$

where the variables $U_{ij}$ are defined on the links of a three-dimensional lattice and $U_{\mathcal{P}}$ is the product of the variables $U_{ij}$ along the links bounding a plaquette $\mathcal{P}$. We introduce a new set of plaquette variables $\{\theta_{\mathcal{P}}\}$ assuming the values 0 or $\pi$, and represent each product $U_{\mathcal{P}}$ as $\cos\theta_{\mathcal{P}}$ [27]. The new variables must satisfy the equation

$$\sum_{\mathcal{P}\in\mathcal{C}}\theta_{\mathcal{P}}=0 \bmod(2\pi), \tag{A2}$$

where the sum is over the plaquettes that form an elementary cell $\mathcal{C}$ of the lattice (which is a cube for the cubic lattice and a tetrahedron or an octahedron for the fcc lattice). In order to understand this constraint, consider the configurations with all $U_{ij}=1$; then (A2) is satisfied. Changing one link $U_{ij}$ always changes two plaquettes' variables $U_{\mathcal{P}}$ of every elementary cell, and therefore (A2) is satisfied for all configurations. Observe that each configuration of $\{U_{\mathcal{P}}\}$ or $\{\theta_{\mathcal{P}}\}$ corresponds to $2^{N_0}$ different configurations of the variables $U_{ij}$, where $N_0$ is the number of the sites of the lattice.

A representation of the partition function (A1) in terms of the variables $\{\theta_{\mathcal{P}}\}$ can be given by introducing another set of Ising variables $\{\tau_i\}$, defined on the cells $\mathcal{C}$, in order to solve the constraint (A2). Then we can write

$$Z(\beta_{\mathcal{P}})=2^{N_0}\sum_{\{\theta_{\mathcal{P}}\}}\prod_{\mathcal{C}}\left[\frac{1}{2}\sum_{\tau_i=\mp1}\exp\left[i(\tau_i-1/2)\sum_{\mathcal{P}\in\mathcal{C}}\theta_{\mathcal{P}}\right]\right]\times\exp\left[\beta_{\mathcal{P}}\sum_{\mathcal{P}}\cos\theta_{\mathcal{P}}\right]. \tag{A3}$$

Now the sum over the variables $\theta_{\mathcal{P}}$ can be performed, giving the result

$$Z(\beta_{\mathcal{P}})=\frac{2^{N_0}}{2^{N_C}}\sum_{\{\tau_i\}}\prod_{\langle ij\rangle}\left[e^{\beta_{\mathcal{P}}}+\tau_i\tau_j e^{-\beta_{\mathcal{P}}}\right], \tag{A4}$$

where the product is over all the couples of elementary cells with a common plaquette, or, equivalently, over the links of the dual lattice. $N_{\mathcal{C}}$ is the number of cells or dual sites. Finally, the formula (A4) can be rewritten as

$$Z(\beta_{\mathcal{P}})=\frac{2^{N_0}}{2^{N_{\mathcal{C}}}}(2\sinh 2\beta_{\mathcal{P}})^{N_{\mathcal{P}}/2}\sum_{\{\tau_i\}}\exp\left[\tilde{\beta}_{\mathcal{P}}\sum_{\langle ij\rangle}\tau_i\tau_j\right], \tag{A5}$$

which is the partition function of an Ising model on the dual lattice, where

$$\tilde{\beta}_{\mathcal{P}}=-\tfrac{1}{2}\ln\tanh\beta_{\mathcal{P}}. \tag{A6}$$

A similar procedure can be used to express on the dual lattice quantities like

$$\sum_{\{U\}}\exp\left[\beta_{\mathcal{P}}\sum_{\mathcal{P}}U_{\mathcal{P}}\right]\prod_{\mathcal{P}'}U_{\mathcal{P}'}, \tag{A7}$$

where $\{\mathcal{P}'\}$ is a set of plaquettes. The only difference with respect to above is that now, for each dual link $\langle lm\rangle$ of a plaquette of the set $\{\mathcal{P}'\}$, we get

$$e^{\beta_{\mathcal{P}}}-\tau_l\tau_m e^{-\beta_{\mathcal{P}}} \tag{A8}$$

instead of the quantity in square brackets of the Eq. (A4). In the end we have the result

$$\sum_{\{U\}}\exp\left[\beta_{\mathcal{P}}\sum_{\mathcal{P}}U_{\mathcal{P}}\right]U_{\mathcal{P}'}=\frac{2^{N_0}}{2^{N_{\mathcal{C}}}}(2\sinh 2\beta_{\mathcal{P}})^{N_{\mathcal{P}}/2}\sum_{\{\tau_i\}}\exp\left[-\tilde{\beta}_{\mathcal{P}}\tau_l\tau_m+\tilde{\beta}_{\mathcal{P}}\sum_{\langle ij\rangle\neq\langle lm\rangle}\tau_i\tau_j\right]. \tag{A9}$$

This proves (2.3).

## APPENDIX B: MEAN-FIELD APPROXIMATION FOR ISING MODELS ON THE DUAL LATTICE OF THE fcc LATTICE

In Sec. III the gauge-Higgs model on the fcc lattice has been related, at small $\beta_1$, to spin models on the dual lattice of the fcc lattice. Here we will use a mean-field approximation to give estimates of the critical points in these models.

The model (3.1) at $\beta_1=0$ can be represented on the dual lattice as an Ising model with only nearest-neighbor interactions (see Appendix A). Its approximated free energy is given by

$$\frac{\Gamma}{k_B T} = -\tilde{\beta}_3 \sum_{\langle ij \rangle} m_i m_j + \sum_i \left[ \frac{1+m_i}{2} \ln(1+m_i) + \frac{1-m_i}{2} \ln(1-m_i) \right] , \tag{B1}$$

where $\tilde{\beta}_3 = -\frac{1}{2} \ln \tanh \beta_3$ and $m_i$ is the approximated thermal average of $s_i$. We will consider the minima of (B1) with $m_i = m^{(4)}$ if the site has coordination 4 and $m_i = m^{(8)}$ if the site has coordination 8 (see Fig. 5). Therefore the free energy $\gamma$ per dual cell can be written as

$$\frac{\gamma}{k_B T} = -8\tilde{\beta}_3 m^{(4)} m^{(8)} + 2S(m^{(4)}) + S(m^{(8)}) , \tag{B2}$$

where $S(m) = \frac{1}{2}[(1+m)\ln(1+m) + (1-m)\ln(1-m)]$. This free energy develops a minimum at $m^{(4)}$, $m^{(8)} \neq 0$, when the determinant of the second derivatives is zero. This condition gives a second-order transition at $\tilde{\beta}_3 = \frac{1}{4}\sqrt{2}$.

At small values of $\beta_1$, the model (3.1) can be mapped on the spin model defined by the Hamiltonian (3.4), whose mean-field free energy is given by

$$\begin{aligned} \frac{\gamma}{k_B T} = & -8[\tilde{\beta}_3^{\text{eff}} - \tfrac{15}{2} \mathcal{C}\mathcal{S}(\tanh\beta_1)^4] m^{(4)} m^{(8)} \\ & - 12\mathcal{S}^2(\tanh\beta_1)^4 (m^{(4)})^2 - 6\mathcal{S}^2(\tanh\beta_1)^4 (m^{(8)})^2 \\ & - 12(\tanh\beta_1)^4 \mathcal{S}^2 (m^{(4)} m^{(8)})^2 \\ & + 2S(m^{(4)}) + S(m^{(8)}) \end{aligned} \tag{B3}$$

with a continuous transition at

$$\tilde{\beta}_3^{\text{eff}} = \frac{1}{4\sqrt{2}} - \frac{3}{\sqrt{2}} \mathcal{S}^2 (\tanh\beta_1)^4 + \tfrac{15}{2} \mathcal{C}\mathcal{S} (\tanh\beta_1)^4 , \tag{B4}$$

where $\mathcal{C} = \cosh 2\tilde{\beta}_3^{\text{eff}}$ and $\mathcal{S} = \sinh 2\tilde{\beta}_3^{\text{eff}}$. This equation can be easily solved at the order $(\tanh\beta_1)^4$, giving, in terms of the original parameters, the critical line

$$\beta_3 \approx -(\tanh\beta_1)^3 - \tfrac{1}{2} \ln \tanh \left[ \frac{1}{4\sqrt{2}} - \frac{3}{\sqrt{2}} \mathcal{S}^2 (\tanh\beta_1)^4 + \tfrac{15}{2} \mathcal{C}\mathcal{S} (\tanh\beta_1)^4 \right] . \tag{B5}$$

The condition for the tricritical point in the case of a classical potential depending on two variables can be found in [28], and is given by

$$0 = \gamma_{4y} \gamma_{2x}^3 + \gamma_{4x} \gamma_{xy}^2 \gamma_{2y} + 6\gamma_{2x2y} \gamma_{2x} \gamma_{xy}^2 , \tag{B6}$$

where $\gamma_x \equiv \partial\gamma / \partial m^{(4)}$, $\gamma_y \equiv \partial\gamma / \partial m^{(8)}$, etc., with all the derivatives calculated at the origin. The solution of the explicit expression of Eq. (B6) gives a tricritical point along the line (B5) at $\beta_1 = 0.745$.


[1] F. Wegner, J. Math. Phys. **12**, 2259 (1971).
[2] *Statistical Mechanics of Membranes and Surfaces,* edited by D. R. Nelson, T. Piran, and S. Weinberg (World Scientific, Singapore, 1989).
[3] *Physics of Amphiphilic Layers,* edited by J. Meunier, D. Langevin, and N. Boccara (Springer-Verlag, Berlin, 1987).
[4] L. E. Scriven, Nature **263**, 123 (1976).
[5] For microemulsions see, e.g., H. T. Davis, J. F. Bodet, L. E. Scriven, and W. G. Miller, in *Physics of Amphiphilic Layers* (Ref. [3]).
[6] As regards bilayers, see, e.g., G. Porte, J. Marignan, P. Basserau, and R. May, J. Phys. (Paris) **49**, 511 (1988).
[7] A. Cappi. P. Colangelo, G. Gonnella, and A. Maritan, Nucl. Phys. B **370**, 659 (1992).
[8] P. Colangelo, G. Gonnella, and A. Maritan, Phys. Rev. E **47**, 411 (1993).
[9] Lattice gauge theories are discussed in J. Kogut, Rev. Mod. Phys. **51**, 659 (1979).
[10] G. A. Jongeward, J. D. Stack, and C. Jayaprakash, Phys. Rev. D **21**, 3360 (1980).
[11] For a review, see J. M. Drouffe and J. B. Zuber, Phys. Rep. **102**, 1 (1983).
[12] D. A. Huse and S. Leibler, Phys. Rev. Lett. **66**, 437 (1991).
[13] G. Bhanot and M. Creutz, Phys. Rev. B **22**, 3370 (1980).
[14] G. Gonnella and A. Maritan, Phys. Rev. B **48**, 932 (1993).
[15] See, e.g., C. Domb, in *Phase Transition and Critical Phenomena,* edited by C. Domb and M. S. Green (Academic, London, 1974), Vol. 3, p. 425.
[16] K. G. Wilson, Phys. Rev. D **10**, 2445 (1974).
[17] See, e.g., R. Savit, Rev. Mod. Phys. **52**, 453 (1980).
[18] E. Fradkin and S. H. Shenker, Phys. Rev. D **19**, 3682 (1979).
[19] R. Balian, J. M. Drouffe, and C. Itzykson, Phys. Rev. D **11**, 2098 (1975).
[20] S. Elitzur, Phys. Rev. D **12**, 3978 (1975).
[21] H. W. J. Blöte and J. Heringa (private communication).
[22] See, e.g., N. W. Ashcroft and N. D. Mermin, *Solid State Physics* (Holt-Saunders International Editions, New York, 1976), Chap. 4.
[23] F. David, Europhys. Lett. **9**, 575 (1989).
[24] A. Pelizzola (private communication).
[25] D. Roux, M. E. Cates, U. Olsson, R. C. Ball, F. Nallet, and A. M. Bellocq, Europhys. Lett. **11**, 4174 (1990).
[26] For a review see G. Porte, J. Phys. Condens. Matter. **4**, 8649 (1992); D. Roux, C. Coulon, and M. E. Cates, J. Phys. Chem. **96**, 4174 (1992).
[27] J. J. M. Rijpkema, Ph.D. thesis, University of Nijmegen, 1984 (unpublished).
[28] J. T. Bartis, J. Chem. Phys. **59**, 5423 (1973).